

Amide proton transfer (APT) MR signal as a novel imaging biomarker for charactering radiation necrosis in rats

S. Wang¹, E. Tryggstad², M. Armour², E. Ford², T. Zhou¹, K. Yan¹, Z. Wen¹, P. C. van Zijl^{1,3}, and J. Zhou^{1,3}

¹Radiology, Johns Hopkins University School of Medicine, Baltimore, MD, United States, ²Radiation Oncology, Johns Hopkins University School of Medicine, Baltimore, MD, United States, ³F.M. Kirby Research Center for Functional Brain Imaging, Kennedy Krieger Institute

Introduction: Radiation therapy of brain tumors may induce radiation necrosis, a well-known delayed side effect in the clinic. Standard MRI (FLAIR as well as contrast-enhanced) cannot distinguish between radiation necrosis and viable tumors in the clinic.¹ Amide proton transfer (APT) imaging provides a unique molecular MRI signal that is based on amide protons of endogenous mobile proteins and peptides in the cytoplasm.² APT was recently shown to be able to separate radiation damage from tumor.³ The propose of this study is to assess APT-MRI characteristics of radiation-induced necrosis in the pre-clinical model and compare the results with several other standard and advanced MRI techniques.

Materials and methods: Eighteen adult rats (Fischer 344; 8-10 weeks) were irradiated with a single, well-collimated x-ray beam in a single dose of 40 Gy to a 10 × 10 mm² region in the left hemisphere. The rats were monitored with anatomical MR imaging monthly until radiation necrosis was found. Imaging experiments were performed on a 4.7T animal MR system (matrix = 64×64, FOV = 32×32 mm², slice thickness = 1.5 mm), using following sequences: T2W (TR/TE = 3s/64ms); T1 map (TE/TI = 30ms/0.05-3.5s); T2 map (TR/TE = 3s/30-90ms), isotropic ADC map (TR/TE = 3s/80ms, b-values = 0-1000s/mm², NA = 8); ASL map (3s labeling at a distance 20 mm away from the imaging slice, TR/TE = 6s/28.6ms, NA = 8); MTR map (RF saturation frequency offset of 10ppm); APT (TR/TE = 10s/30ms, offsets of ±3.5 ppm with respect to water, NA = 16); and gadolinium-enhanced T1W (TR/TE = 700ms/10ms). The ROIs for quantitative analysis included a central necrotic area, a peri-necrotic region, and contralateral gray matter (caudate putamen).

Results: Conventional MRI features: Radiation necrosis showed heterogeneous on the T2W image and gadolinium enhancement on the post-contrast T1W image, an appearance similar to the characteristics of viable brain tumor or tumor recurrence. **Advanced MRI features:** Although radiation necrosis was heterogeneously hyperintense on the T1, T2, and MTR maps, it was particularly interesting that the lesion on the ADC, blood flow, and APT maps (Fig. 1) consisted of a hypointense central zone and a peripheral zone with unique signal intensities that depended on the sequence. On the ADC map, the peripheral zone was highly hyperintense. On the blood flow map, blood flow decreased in most irradiated hemisphere, and it was slightly hyperintense in the peripheral zone, compared with surrounding brain tissue. On the APT map, the peripheral zone was iso-intense to slightly hyperintense, compared with the contralateral gray matter. **Quantitative MRI analysis:** There were significantly higher ADC values in the peri-necrotic regions than in the contralateral gray matter (p < 0.01; Table 1). The APT signal intensity of the necrotic core was significantly lower than that of the contralateral gray matter (p < 0.01). It seemed that the APT signal intensity of the peri-necrotic region was higher than that of the contralateral gray matter, but no significant difference was found. **Histology:** As shown in Fig. 2, the necrotic core was correlated with parenchymal coagulative necrosis and fibrosis (the cardinal histology characteristic of radiation necrosis). In the peri-necrotic region, there was reactive brain tissue, including reactive gliosis, vascular wall thickness and hemorrhage.

Discussion: The APT-MRI signal of radiation necrosis is hypointense in the necrotic core and iso-intense to slightly hyperintense in the peri-necrotic region, compared to the contralateral gray matter. Histology proves that the central zone and peri-necrotic region are correlated with coagulate necrosis and reactive brain tissue, respectively. **Based on these, in a more complicated tissue structure, where the necrotic core and peri-necrotic region co-exist, as observed in the clinic, the average ADC may become hypointense, iso-intense, or hyperintense; however, the APT signal would be consistently hypointense.** When comparing with other MRI techniques, APT imaging may improve the accuracy in the differential diagnosis between radiation necrosis and tumor recurrences in patients.

¹Yang et al. *Nat. Rev. Clin. Oncol.* 6, 648(2009). ²Zhou et al. *Nat. Medicine* 9, 1085 (2003). ³Zhou et al. *Nat. Medicine* In press.

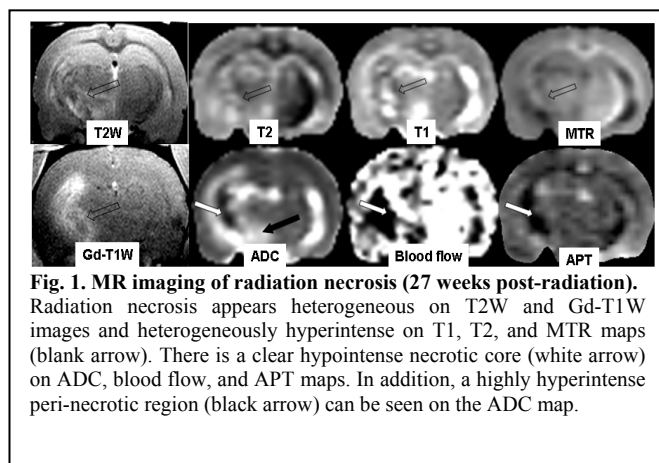


Fig. 1. MR imaging of radiation necrosis (27 weeks post-radiation). Radiation necrosis appears heterogeneous on T2W and Gd-T1W images and heterogeneously hyperintense on T1, T2, and MTR maps (blank arrow). There is a clear hypointense necrotic core (white arrow) on ADC, blood flow, and APT maps. In addition, a highly hyperintense peri-necrotic region (black arrow) can be seen on the ADC map.

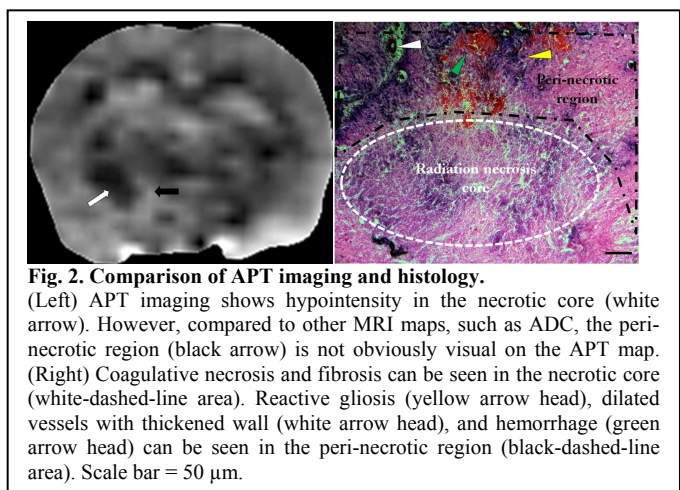


Fig. 2. Comparison of APT imaging and histology. (Left) APT imaging shows hypointensity in the necrotic core (white arrow). However, compared to other MRI maps, such as ADC, the peri-necrotic region (black arrow) is not obviously visual on the APT map. (Right) Coagulative necrosis and fibrosis can be seen in the necrotic core (white-dashed-line area). Reactive gliosis (yellow arrow head), dilated vessels with thickened wall (white arrow head), and hemorrhage (green arrow head) can be seen in the peri-necrotic region (black-dashed-line area). Scale bar = 50 μm.

Table 1: Quantitative multi-parametric MRI analysis of radiation necrosis (n = 18)

	T1 (s)	T2 (ms)	MTR (%)	ADC (10 ⁻⁹ m ² /s)	Blood flow (ml/100g/min)	APT (%)
Radiation necrosis core	1.40 ± 0.21	58.3 ± 8.4	42.08 ± 25.84	0.82 ± 0.23	33.8 ± 77.5***	-3.49 ± 0.97**
Peri-necrotic region	1.45 ± 0.19	59.8 ± 6.8	40.19 ± 26.40	1.10 ± 0.29**	65.2 ± 73.0*	-1.44 ± 1.19
Contral. gray matter	1.31 ± 0.15	54.8 ± 6.6	45.37 ± 24.29	0.83 ± 0.22	139.0 ± 108.6	-2.13 ± 0.76

The differences between necrotic core and contralateral gray matter or between peri-necrotic region and contralateral gray matter were compared by one-way ANOVA post-hoc Turkey's test. *, p < 0.05; **, p < 0.01; ***, p < 0.001.